IOWA STATE UNIVERSITY
Digital Repository

Mechanical Engineering Publications | Mechanical Engineering

12-2014

Dual-pump vibrational/rotational femtosecond/picosecond coherent anti-Stokes Raman scattering temperature and species measurements

Chloe Elizabeth Dedic
Iowa State University, cededic@iastate.edu

Joseph D. Miller
Air Force Research Laboratory

Terrence R. Meyer
Iowa State University, trm@iastate.edu

Follow this and additional works at: http://lib.dr.iastate.edu/me_pubs

Part of the Mechanical Engineering Commons

The complete bibliographic information for this item can be found at http://lib.dr.iastate.edu/me_pubs/172. For information on how to cite this item, please visit http://lib.dr.iastate.edu/howtocite.html.

This Article is brought to you for free and open access by the Mechanical Engineering at Iowa State University Digital Repository. It has been accepted for inclusion in Mechanical Engineering Publications by an authorized administrator of Iowa State University Digital Repository. For more information, please contact digirep@iastate.edu.

Dual-pump vibrational/rotational femtosecond/ picosecond coherent anti-Stokes Raman scattering temperature and species measurements

Abstract
A method for simultaneous ro-vibrational and pure-rotational hybrid femtosecond/picosecond coherent anti-Stokes Raman scattering (fs/ps CARS) is presented for multi-species detection and improved temperature sensitivity from room temperature to flame conditions. N_2/CH_4 vibrational and $N_2/O_2/H_2$ rotational Raman coherences are excited simultaneously using fs pump pulses at 660 and 798 nm, respectively, and a common fs Stokes pulse at 798 nm. A fourth narrowband 798 nm ps pulse probes all coherence states at a time delay that minimizes nonresonant background and the effects of collisions. The transition strength is concentration dependent, while the distribution among observed transitions is related to temperature through the Boltzmann distribution. The broadband excitation pulses and multiplexed signal are demonstrated for accurate thermometry from 298 to 2400 K and concentration measurements of four key combustion species.

Keywords
Boltzmann equation, optical pumping, Raman scattering, Raman spectroscopy, time delay, broadband excitation, coherent anti-Stokes Raman scattering, concentration measurement, effects of collisions, temperature sensitivity

Disciplines
Mechanical Engineering

Comments
This article is from *Optics Letters* 39 (2014): 6608, doi: 10.1364/OL.39.006608. Posted with permission.

Rights
This paper was published in Optics Letters and is made available as an electronic reprint with the permission of OSA. The paper can be found at the following URL on the OSA website: https://www.osapublishing.org/ol/abstract.cfm?uri=ol-39-23-6608. Systematic or multiple reproduction or distribution to multiple locations via electronic or other means is prohibited and is subject to penalties under law.

This article is available at Iowa State University Digital Repository: http://lib.dr.iastate.edu/me_pubs/172

Dual-pump vibrational/rotational femtosecond/picosecond coherent anti-Stokes Raman scattering temperature and species measurements

Chloe E. Dedic,[1] Joseph D. Miller,[2] and Terrence R. Meyer[1,*]

[1]*Iowa State University, Department of Mechanical Engineering, Ames, Iowa 50011, USA*

[2]*Air Force Research Laboratory, Aerospace Systems Directorate, Wright-Patterson AFB, Ohio 45431, USA*

**Corresponding author: trm@iastate.edu*

Received September 19, 2014; accepted October 16, 2014;
posted October 20, 2014 (Doc. ID 222788); published November 18, 2014

A method for simultaneous ro-vibrational and pure-rotational hybrid femtosecond/picosecond coherent anti-Stokes Raman scattering (fs/ps CARS) is presented for multi-species detection and improved temperature sensitivity from room temperature to flame conditions. N_2/CH_4 vibrational and $N_2/O_2/H_2$ rotational Raman coherences are excited simultaneously using fs pump pulses at 660 and 798 nm, respectively, and a common fs Stokes pulse at 798 nm. A fourth narrowband 798 nm ps pulse probes all coherence states at a time delay that minimizes nonresonant background and the effects of collisions. The transition strength is concentration dependent, while the distribution among observed transitions is related to temperature through the Boltzmann distribution. The broadband excitation pulses and multiplexed signal are demonstrated for accurate thermometry from 298 to 2400 K and concentration measurements of four key combustion species. © 2014 Optical Society of America

OCIS codes: (300.6230) Spectroscopy, coherent anti-Stokes Raman scattering; (320.7150) Ultrafast spectroscopy; (120.1740) Combustion diagnostics; (300.6290) Spectroscopy, four-wave mixing.
http://dx.doi.org/10.1364/OL.39.006608

Coherent anti-Stokes Raman scattering (CARS) spectroscopy has been used extensively for accurate, *in-situ* temperature and relative species concentration measurements in gas-phase samples to increase the understanding of chemical reactions pertinent to complex combustion processes [1]. Early efforts implemented CARS using nanosecond (ns) sources to excite vibrational or pure-rotational molecular transitions. To excite multiple species simultaneously, dual-broadband CARS was developed to study closely spaced Raman transitions using two broadband dye lasers [2]. Another technique, dual-pump CARS, uses two separate narrowband pump beams that can be tuned to excite a variety of molecule pairs [3]. Bengtsson *et al.* combined vibrational CARS and dual-broadband CARS to simultaneously excite and detect ro-vibrational and pure-rotational spectra [4]. This work was expanded on by Roy *et al.* to excite pure-rotational spectra of N_2 and O_2 and ro-vibrational spectra of N_2 and CO_2 to measure concentration and temperature within low- and high-temperature regions [5]. Tedder *et al.* increased the spectral excitation bandwidth using a unique mixture of laser dye to measure seven species within H_2/C_2H_4 combustion mixtures [6]. Recently, Satija and Lucht utilized a two-beam configuration to generate pure-rotational CARS and a third beam to probe N_2 ro-vibrational CARS, offering temperature measurements over a broad range using a simplified setup [7].

Challenges associated with ns CARS temperature and species measurements include low laser repetition rates, uncertainties due to nonresonant background [8], and collisional broadening at elevated pressures [9]. To isolate the resonant CARS signal from nonresonant background, picosecond [10] and femtosecond [11] laser sources have been used to temporally separate the probe and preparation pulses. To avoid complex coherent interferences that occur with broadband femtosecond excitation/detection of multiple species, an approach that combines broadband, femtosecond excitation with narrowband, picosecond detection has been employed. This approach, hybrid femtosecond/picosecond (fs/ps) CARS, can be used to enhance chemical specificity [12,13], simplify spectral analysis, suppress nonresonant background, and reduce the effects of collisions for accurate thermometry from low to high pressures [14].

Hybrid fs/ps CARS has been used to probe the vibrational transitions of N_2 for high-speed measurements of temperature with a precision of 2.2% and error of 3.3% [15], but is limited to temperatures above ~1200 K due to low population of the N_2 hot bands. Additionally, pure-rotational CARS has been implemented to measure temperature with errors of 1.8% and 2.5% at 1400 and 2283 K, respectively, with spectral focusing and second-harmonic bandwidth compression of the ps probe [16]. Measurements of relative species concentrations have been accomplished using rotational or vibrational transitions of N_2/O_2 [16,17] or N_2/CH_4 [18], respectively, and the ability to excite multiple species, such as N_2, H_2, CH_4, and CO_2, has been demonstrated using ultra-broadband CARS with a supercontinuum source [19].

In this Letter, quantitative measurement of four species (N_2, O_2, CH_4, and H_2) is demonstrated along with thermometry over a wide range from 298 to 2300 K through simultaneous pure-rotational and ro-vibrational hybrid fs/ps CARS. The ability to measure multiple species concentrations and wide temperature variations with minimal interferences from nonresonant background and collisions is important in unsteady combustion and other gas-phase reacting flows. This approach can furthermore be expanded to include additional species by utilizing laser sources with significantly wider spectral bandwidth.

Hybrid fs/ps CARS is a nonlinear, four-wave-mixing process that utilizes 100-fs pump/Stokes pulses (ω_p/ω_s) to excite vibrational and/or rotational transitions of a

 © 2014 Optical Society of America

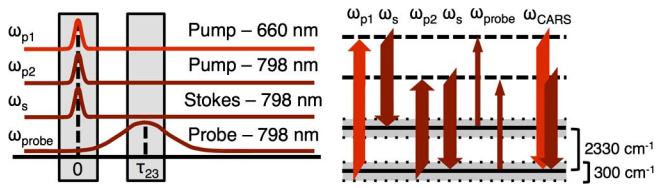

Fig. 1. CARS timing and frequency diagrams.

sample molecule. A third, frequency-narrowed picosecond pulse (ω_{probe}) is used to probe the molecular response. Simultaneous excitation of vibrational and rotational Raman coherences is accomplished using one Stokes beam, ω_s, at 798 nm and two pump beams, ω_{p1} and ω_{p2}, at 660 and 798 nm, respectively. A narrowband pulse, ω_{probe}, at 798 nm is used to probe both Raman coherences and is delayed in time to suppress nonresonant interferences. The resulting frequency-resolved CARS signals contain ro-vibrational spectra and pure-rotational spectra. This configuration is shown in the time domain in Fig. 1(a) and frequency domain in Fig. 1(b).

Figure 1 only displays the excitation of vibrational and rotational N_2 transitions, but the same pulse arrangement also excites pure-rotational transitions of O_2, the $S(0)$ pure-rotational transition of H_2 at 354 cm^{-1}, and the ν_1 vibrational transition of CH_4 at 2914 cm^{-1} because of the broadband pulses used. The frequency difference between the 660 nm pump and 798 nm Stokes pulses is centered between the N_2 and CH_4 Q-branch transitions [18].

As discussed by Engel *et al.* [18], the molecular number density can be related to the CARS signal by Eq. (1) for well-separated transitions:

$$N_i \propto \frac{\sqrt{I_{\text{CARS}}|_i}}{A_i \sqrt{I_{\text{NR}}|_i \left(\frac{d\sigma}{d\Omega}\right)_i}}. \tag{1}$$

Here, $I_{\text{CARS}}|_i$ is the CARS intensity of species i, A_i is an experimental constant, and $(d\sigma/d\Omega)_i$ is the relative Raman cross section. $I_{\text{NR}}|_i$ represents the excitation efficiency of species i since the excitation energy has the same spectral characteristics as the nonresonant CARS intensity as measured within a cell of argon. For a mixture of n species, the mole fraction of species i can be described by

$$x_i = \frac{N_i}{\sum_{j=1}^{n} N_j}. \tag{2}$$

Combining Eqs. (1) and (2) and consolidating the excitation energy, the Raman cross section, and the experimental constant for each species into constants K_i, which can be determined based on a calibration curve, the measured mole fraction for one species is defined by

$$x_i = \frac{K_i \sqrt{I_{\text{CARS}}|_i}}{\sum_{j=1}^{n-1} K_j \sqrt{I_{\text{CARS}}|_j} + \sqrt{I_{\text{CARS}}|_n}}. \tag{3}$$

In this work, Eq. (3) is used to calculate mole fractions of CH_4 and H_2 within a mixture of N_2, CH_4, and H_2. To relate CH_4 to H_2, which are simultaneously excited but collected separately, Q-branch transitions are normalized to the $\nu(N_2)$ transition, and S-branch transitions are normalized to the $N_2(J = 8)$ transition. Because N_2 is nearly inert in combustion reactions, it is an excellent candidate to relate species detected separately. The measurement of O_2 mole fraction within a mixture of N_2 and O_2 is also achieved utilizing Eq. (3). In addition, a method for measuring mole fraction with non-isolated N_2/O_2 lines is also investigated for enhancing accuracy at low O_2 mole fractions and for use when isolated lines are unavailable.

In addition to mole fraction, temperature is measured using vibrational and rotational CARS spectra. A time- and frequency-resolved model based on fundamental spectroscopic constants and experimental parameters was used to generate N_2 ro-vibrational and N_2/O_2 rotational spectra at various temperatures as implemented by Miller and co-workers [15,20] and described in detail by Stauffer *et al.* [21] and Prince *et al.* [12]. Best-fit temperatures were computed using a spectral library and optimization algorithm to minimize the residual between experimental and modeled spectra.

The experimental arrangement is modified from previously published studies [15,20]. A Ti:sapphire, regeneratively amplified, 1-kHz-rate laser (Solstice, Spectra-Physics) is used to produce a 2.5 mJ, 150 cm^{-1}, 100 fs pulse centered around 798 nm. 1.5 mJ is directed into a variable-bandwidth 4-f pulse shaper. The output, ω_{probe}, is used as the probe pulse for both rotational and vibrational fs/ps CARS. During this work, a 2.5 cm^{-1} Gaussian probe pulse was selected to provide sufficient spectral resolution for rotational CARS and adequate energy to perform vibrational CARS at high temperature.

The remaining 1 mJ from the source is used to pump an optical parametric amplifier (TOPAS, Spectra-Physics). The output of the OPA is frequency doubled using a second-harmonic-generation crystal, and the wavelength can be tuned to excite transitions of multiple molecules as the vibrational pump pulse, ω_{p1}. The residual of the OPA is split using a 50/50 beam splitter. One-half of the beam is used as the Stokes pulse, ω_s, while the other half is used as the rotational CARS pump beam, ω_{p2}. The frequency difference between ω_{p1} and ω_s corresponds to vibrational transitions of N_2 and CH_4, and the difference between ω_{p2} and ω_s corresponds to pure-rotational transitions of N_2, O_2, and H_2. A BOXCARS phase-matching configuration is used, with the two pump beams, ω_{p1} and ω_{p2}, aligned collinearly. The probe pulse is delayed in time (τ_{23}) relative to the preparation pulses to suppress nonresonant background. The resulting collinear pure-rotational and ro-vibrational CARS signals can be directed to a 0.303 m spectrometer (Shamrock SR-3031, Andor) and resolved separately using a 1200 line/mm grating and an electron-multiplied CCD camera (DU-970 P-UVB, Newton).

The simultaneous dual-pump vibrational/rotational fs/ps CARS technique was used to measure mole fractions of CH_4 and H_2 in a $CH_4/H_2/N_2$ mixture within a 298 K flow cell. The same cell was used to study a binary mixture of O_2 and N_2 at concentrations simulating O_2

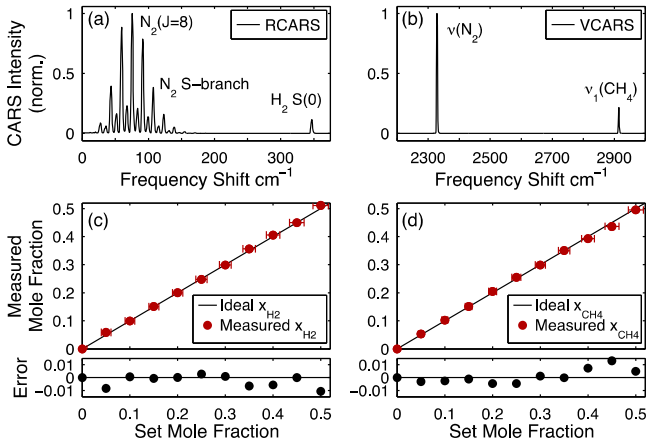

Fig. 2. Sample (a) H_2/N_2 spectra, (b) CH_4/N_2 spectra, and measured mole fractions of (c) H_2 and (d) CH_4.

consumption during a reaction. To test the system capability for thermometry, CARS measurements were performed within the product stream of an adiabatic H_2–air Hencken burner flame over a range of fuel/air equivalence ratios (60 SLPM typical H_2–air flow rate).

Figure 2 shows sample CARS spectra recorded within a mixture of 50% N_2, 30% H_2, and 20% CH_4 at a probe delay of 12 ps. As discussed earlier, the intensities of the $\nu_1(CH_4)$ and $\nu(N_2)$ vibrational transitions and the $N_2(J = 8)$ and H_2 $S(0)$ pure-rotational transitions be used to calculate the respective mole fractions. Figure 2 also displays the measured mole fractions versus the set mole fractions of H_2 and CH_4. The horizontal error bars represent the uncertainty of the set mole fractions attributable to the mass-flow controllers. The experimental constant, K, for H_2 and CH_4 is 1.82 and 0.92, respectively. The absolute error associated with the concentration measurement is shown at the bottom of Fig. 2 and is less than 0.011 for H_2 and 0.013 for CH_4 for mole fractions between 0.05 and 0.50.

Due to the well-separated nature of the $\nu_1(CH_4)$ and $\nu(N_2)$ transitions and the $N_2(J = 8)$ and H_2 $S(0)$ transitions, measuring mole fractions of CH_4, H_2, and N_2 within a gas mixture is relatively straightforward. However, O_2 and N_2 rotational transitions are spectrally overlapped at atmospheric conditions, resulting in a complex spectrum. Frequency beating between overlapping transitions can be observed by delaying the probe pulse in time, as highlighted by the experimental time-frequency plot in Fig. 3(a). For the purposes of this study the probe was set to a fixed delay of 12.5 ps [Fig. 3(a) red line], and the resulting spectra at varying concentrations of O_2 and N_2 are shown in Fig. 3(b). Initially the gas cell was filled with air [Fig. 3(b) dark blue line plot] and the N_2 concentration was increased incrementally until the cell contained 100% N_2 [Fig. 3(b) red dashed line plot]. This concentration range spans typical combustion conditions. The line positions for N_2 and O_2 S-branch transitions were calculated and are shown in Fig. 3(c).

The following analysis demonstrates two methods for measuring the O_2 concentration. To calculate O_2 mole fractions similar to the previous calculations for CH_4 and H_2, well-separated N_2 and O_2 transitions must be

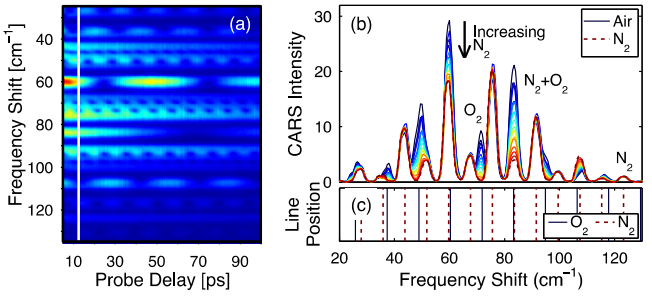

Fig. 3. (a) Experimental time-frequency plot of_fs/ps RCARS in air at 298 K, (b) RCARS spectra of N_2/O_2 at time delay indicated by white line in (a) normalized to the $N_2(J = 14)$ transition with concentrations varying from air to pure N_2, and (c) calculated N_2/O_2 line positions.

available. As evident from the line positions in Fig. 3(c), a separated $N_2(J = 14)$ transition exists near 123 cm^{-1}. This transition can be considered separated because its intensity decays as a simple exponential function in time. In Fig. 3(b) all spectra are normalized to this transition. There is a near-separated $O_2(N = 11)$ transition at 72 cm^{-1}, but its response is an exponential decay with an oscillating amplitude, indicating slight overlap with the adjacent N_2 transitions. However, this transition was compared to the $N_2(J = 14)$ line, and Eq. (3) was used to calculate O_2 mole fraction. The results of this calculation for O_2 mole fractions up to 0.21 are shown in Fig. 4(a), where K_{O_2} is 0.08 and the horizontal error bars associated with uncertainty of the set mole fractions are within the symbols. The measurement error is better than 0.011 for O_2 mole fractions greater than 0.04 but increases substantially at lower concentrations.

Mole fraction information can also be found by considering the nearly overlapped $O_2(N = 13)$ and $N_2(J = 9)$ transitions near 83.5 cm^{-1}, with a central frequency separation of 0.2 cm^{-1}. As shown in Fig. 3(b), the transition from air to pure N_2 results in a simple decrease in the line intensity with no appreciable shift in the peak spectral location or change in line shape. This mixed spectral feature was compared to the $N_2(J = 14)$ line and the result as a function of theoretical mole fraction is shown in Fig. 4(b). These results fit well to a second-order polynomial, as indicated in Eq. (4), where p_1, p_2, and p_3 are coefficients determined using a least squares fitting routine and R is defined in Eq. (5). This relationship can be used as a secondary method of measuring O_2 mole fraction with reduced error at low mole fractions:

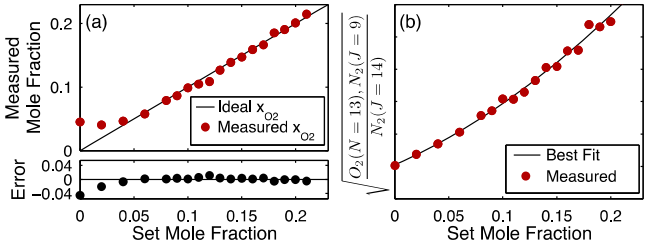

Fig. 4. (a) Measured O_2 mole fraction calculated from a nearly isolated O_2 transition. (b) Calibration curve shown with polynomial fit for overlapped N_2 and O_2 transitions.

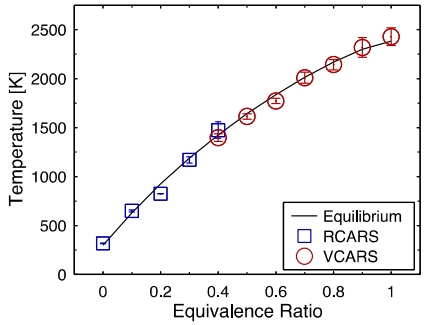

Fig. 5. Equivalence ratio curve showing the temperature fitting results for RCARS and VCARS compared to the adiabatic flame temperature.

$$x_{O_2} = p_1 R^2 + p_2 R + p_3, \tag{4}$$

$$R = \left(\frac{\sqrt{I_{\mathrm{CARS}}|_{O_2(N=13),N_2(J=9)}}}{\sqrt{I_{\mathrm{CARS}}|_{N_2(J=14)}}} \right). \tag{5}$$

Although the measurement of O_2 mole fraction is shown within a simple binary mixture, this measurement can be performed within a sample of N_2, O_2, CH_4, and H_2 using the same procedure but normalizing all pure-rotational spectra to the well-separated $N_2(J = 14)$ transition.

Dual-pump vibrational/rotational fs/ps CARS was performed within a H_2–air flame for fuel/air equivalence ratios (ϕ) between 0.1 and 1.0 and at room temperature to evaluate the accuracy of the technique for thermometry over a wide range of temperatures. The results of these measurements are shown in Fig. 5; the vertical error bars represent one standard deviation due to the variation of best-fit temperatures for 100 time-averaged spectra. The probe pulse was delayed 7.5 ps from the preparation pulses to minimize nonresonant background and perform the temperature measurement before collisional line broadening becomes significant. The RCARS and VCARS temperature measurements at $\phi = 0.4$ agree within one standard deviation verifying the assumption of rotational and vibrational equilibrium. The solid line represents the calculated adiabatic flame temperature assuming equilibrium-combustion products. Typical accuracies for the temperature range in Fig. 5 are 95% and 98% for RCARS and VCARS measurements, respectively. The larger error in RCARS measurements is due to error in the theoretical modeling of overlapping O_2 and N_2 rotational transitions and requires further evaluation. However, this work demonstrates the feasibility for using dual-pump vibrational/rotational fs/ps CARS for thermometry in combustion environments.

In summary, this Letter demonstrated a dual-pump hybrid fs/ps CARS system that can simultaneously excite ro-vibrational and pure-rotational transitions of multiple molecules. This system can be used to detect vibrational spectra of N_2 and CH_4 and rotational spectra of N_2, O_2, and H_2 for concentration measurements and thermometry over a wide range (298–2400 K). Accuracies are similar to that of ns CARS measurements of single species or over narrower temperature ranges. Moreover, these measurements are insensitive to collisions, independent of nonresonant background, and can be performed with higher repetition-rate laser sources. Future concentration measurements could be extended to include simultaneous vibrational excitation and measurement of CO and CO_2 through the use of a laser source with wider spectral bandwidth. Additionally, simultaneous excitation of ro-vibrational and pure-rotational energy states could be used to explicitly study vibrational–rotational nonequilibrium distributions.

Funding was provided by the Air Force Office of Scientific Research (Dr. Chiping Li, Program Manager) and the National Science Foundation (CBET-1056006, Dr. A. Atreya and R.-H. Chen, Program Directors). C. Dedic was supported by the National Science Foundation Graduate Fellowship Program.

References

1. S. Roy, J. R. Gord, and A. Patnaik, Prog. Energ. Combust. **36**, 280 (2010).
2. A. C. Eckbreth and T. J. Anderson, Appl. Opt. **24**, 2731 (1985).
3. R. P. Lucht, Opt. Lett. **12**, 78 (1987).
4. P.-E. Bengtsson, L. Martinsson, and M. Alden, Appl. Spectrosc. **49**, 188 (1995).
5. S. Roy, T. R. Meyer, R. P. Lucht, M. Afzelius, P.-E. Bengtsson, and J. R. Gord, Opt. Lett. **29**, 1843 (2004).
6. S. A. Tedder, J. L. Wheeler, A. D. Cutler, and P. M. Danehy, Appl. Opt. **49**, 1305 (2010).
7. A. Satija and R. P. Lucht, Opt. Lett. **38**, 1340 (2013).
8. A. C. Eckbreth and R. J. Hall, Combust. Sci. Technol. **25**, 175 (1981).
9. T. Seeger, F. Beyrau, A. Brauer, and A. Leipertz, J. Raman Spectrosc. **34**, 932 (2003).
10. S. Roy, T. R. Meyer, and J. R. Gord, Appl. Phys. Lett. **87**, 264103 (2005).
11. J. R. Gord, T. R. Meyer, and S. Roy, Annu. Rev. Anal. Chem. **1**, 663 (2008).
12. B. D. Prince, A. Chakraborty, B. M. Prince, and H. U. Stauffer, J. Chem. Phys. **125**, 044502 (2006).
13. D. Pestov, R. K. Murawski, G. O. Ariunbold, X. Wang, M. C. Zhi, A. V. Sokolov, V. A. Sautenkov, Y. V. Rostovtsev, A. Dogariu, Y. Huang, and M. O. Scully, Science **316**, 265 (2007).
14. J. D. Miller, C. E. Dedic, S. Roy, J. R. Gord, and T. R. Meyer, Opt. Express **20**, 5003 (2012).
15. J. D. Miller, M. N. Slipchenko, T. R. Meyer, H. U. Stauffer, and J. R. Gord, Opt. Lett. **35**, 2430 (2010).
16. S. P. Kearney, Appl. Opt. **53**, 6579 (2014).
17. S. P. Kearney, D. J. Scoglietti, and C. J. Kliewer, Opt. Express **21**, 12327 (2013).
18. S. R. Engel, J. D. Miller, C. E. Dedic, T. Seeger, A. Leipertz, and T. R. Meyer, J. Raman Spectrosc. **44**, 1336 (2013).
19. A. Bohlin and C. J. Kliewer, Appl. Phys. Lett. **104**, 031107 (2014).
20. J. D. Miller, S. Roy, M. N. Slipchenko, J. R. Gord, and T. R. Meyer, Opt. Express **19**, 15627 (2011).
21. H. U. Stauffer, J. D. Miller, M. N. Slipchenko, T. R. Meyer, B. D. Prince, S. Roy, and J. R. Gord, J. Chem. Phys. **140**, 024316 (2014).